Optical spin polarization and state-sensitive detection of a cesium atomic beam

Bernardo Jaduszliwer and Yat C. Chan
Electronics Technology Center, The Aerospace Corporation, P.O. Box 92957, Los Angeles, California 90009
(Received 16 November 1992)

A cesium atomic beam having a high degree of polarization is prepared by optical pumping with two circularly polarized diode lasers, and a technique for state-sensitive atomic detection involving laser-induced fluorescence in a magnetic field (LIFB) is introduced. An atomic-beam polarization of 93% is measured using the LIFB technique, and the combined use of optical-state preparation and LIFB detection in an atomic-recoil experiment to study spin-changing electron-atom collisions is demonstrated.

PACS number(s): 32.80.−t, 32.60.+i, 34.80.Nz

I. INTRODUCTION

The study of electron-atom collisions is an important tool for the exploration of atomic interactions [1]. The many-body character of atomic processes precludes in most cases the direct application of basic physical laws; theoretical predictions depend on approximations and thus require close comparison with experiment. Scattering experiments, which directly probe the wave function of the collision system, provide very stringent tests of our current theoretical understanding. Many subtle effects in electron-atom collisions depend on the relative spin orientation of the collision partners. In a typical scattering experiment, performed without regard to spin state, those effects are washed out by averaging and summing over the initial and final states of the system, respectively, thus degrading the power of the experiment as a touchstone for theory.

Most electron-atom scattering experiments with spin analysis of the collision system have involved either "light doublet" atoms like hydrogen or the light alkali metals, or else "heavy singlet" atoms like mercury, krypton, or xenon; work in these areas has been reviewed most recently by Kessler [2]. In the first case, that of electrons scattering on a light target having an unpaired valence electron, exchange is the dominant spin-dependent interaction. Relativistic effects such as spin-orbit coupling give rise to spin-polarization effects in the second case, and since the target is a spin-zero atom, these effects are not masked by spin exchange. As a result of these experimental studies, considerable progress has been made in the understanding of those interactions in atomic physics.

A wealth of new physics opens up when exchange and relativistic couplings are both significant. New theoretical tools are required [3] to describe electron-atom collisions under these circumstances, and the presence of two interactions coupling the same initial and final states of the collision system introduces the possibility of interference effects [4]. McClelland, Kelley, and Celotta [5] investigated these effects for electron scattering on sodium, and Jaduszliwer, Bhaskar, and Bederson [6] did so with rubidium. The best choice of target atom for experimental studies of a situation in which both interactions are significant is cesium, which has a high atomic number Z, enhancing relativistic couplings, and is an alkali-metal atom, allowing for the simplest possible treatment of exchange. Baum *et al.* have recently [7] described a spin-polarized cesium atomic-beam system developed at the University of Bielefeld for this purpose; it relies on optical pumping of the cesium atoms for state preparation, and splitting of the beam in a high-field Stern-Gerlach magnet for state analysis.

We have built a spin-polarized cesium-beam apparatus to investigate the role of spin in electron-cesium collisions by the atomic-recoil technique [8] in which postcollisional observations are made on the recoiled atom, rather than on the scattered electron. This apparatus was used to measure electron-cesium total scattering cross sections [9], but since those measurements did not require a spin-polarized atomic beam, we did not discuss the apparatus features involved in beam-spin-state preparation and analysis. We spin-polarize the cesium atomic beam by optical pumping with Al-Ga-As diode lasers; our technique for state-sensitive detection of the atoms uses laser-induced fluorescence in a magnetic field (LIFB). This paper describes our atomic-recoil apparatus, the optical-pumping scheme used to spin-polarize the cesium atomic beam, and the LIFB detection technique; discusses the theoretical analysis required to interpret the LIFB spectra; and presents some results.

II. THE ATOMIC-RECOIL APPARATUS

The atomic-recoil experiments to be performed are shown conceptually in Fig. 1: an effusive oven produces a cesium atomic beam, which is velocity-selected and focused by a hexapole magnet, and spin-polarized by optical pumping with diode lasers. Then, the angular distribution and spin state of cesium atoms recoiled in collisions with electrons are detected by laser-induced fluorescence.

The atomic-beam apparatus built at The Aerospace Corp. to perform those experiments is shown schematically in Fig. 2. The cesium-beam source is a two-chambered effusive oven. The body of the oven is outside the vacuum envelope of the apparatus, providing easy access to the cartridge heaters and temperature-controller

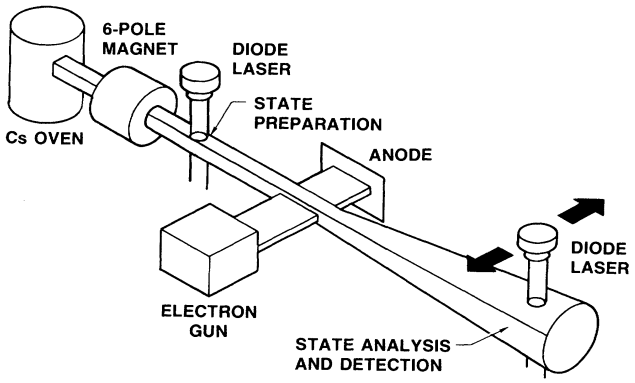

FIG. 1. Experimental concept: A cesium beam is focused and velocity-selected by a hexapole magnet, and spin-polarized by optical pumping with diode lasers. After undergoing collisions with electrons, recoiled atoms are detected by state-sensitive laser-induced fluorescence.

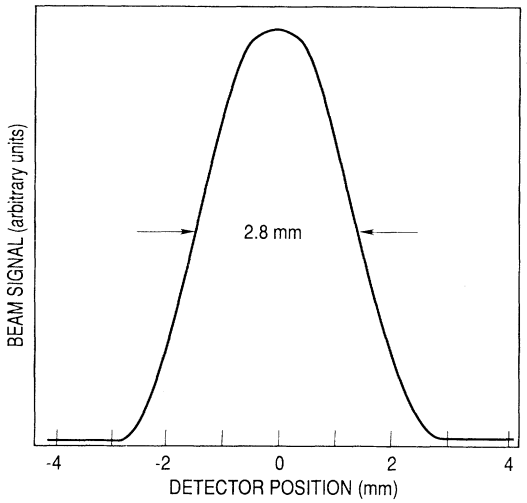

FIG. 3. Cesium-beam transverse-intensity distribution.

thermocouple sensors. A samarium-cobalt hexapole magnet, 2.54 cm in length and 2.54 cm in diameter, with a 0.32-cm-diam bore, manufactured to our specifications by the Brobeck Corp. (Berkeley, CA), is mounted on the front end of the oven to provide velocity selection and beam collimation [10]. A flexible bellows connecting the source assembly to the vacuum envelope allows us to align the source with the axis of the apparatus.

The electron gun, described previously [9], is located at the center of the collision chamber; the interaction region, in which atomic and electron beams overlap, is centered 112 cm away from the oven outlet. The oven is operated normally with the cesium reservoir heated up to 200 °C, and the outlet chamber about 25 °C hotter. Under those conditions, we estimate the cesium-atom density at the interaction region to be 5.5×10^{8} cm^{-3}, with a dimer fraction of less than 0.1% [9].

The atomic-beam intensity is monitored by a conventional surface ionization detector consisting of a 0.013-cm-diam tungsten "hot wire," an accelerating ion lens, and a 90°-sector magnetic ion-mass filter which discriminates against sodium or potassium ions diffusing off the "hot wire." The cesium-ion current is amplified by a high-current Channeltron electron multiplier. The detector assembly is mounted on a flexible bellows, allowing alignment of the detector with the axis of the apparatus. The LIFB detection region is located just in front of the "hot wire," 91.4 cm from the center of the interaction region. The detection chamber rotates about the center of the collision chamber, in the plane defined by the electron and atomic beams. The intensity profile of the detected atomic beam is shown in Fig. 3.

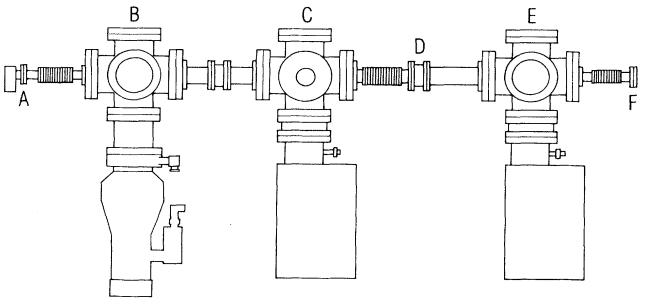

FIG. 2. Schematic diagram of experimental setup: A, cesium beam source; B, state-preparation chamber; C, collision chamber; D, beam drift tube; E, state-sensitive detection chamber; and F, beam monitor.

III. OPTICAL SPIN STATE PREPARATION

Many previous [2] measurements of electron–alkali-metal-atom spin-changing-collision cross sections were performed by spin-selecting atoms in an inhomogeneous magnetic field. Typically, magnetic spin selection is performed in a high magnetic field, where the electron and nuclear magnetic moments couple independently to the external field. Under these conditions, the atomic beam splits into two components having $m_J=\pm\frac{1}{2}$, respectively. If the collision experiment is also performed in a high magnetic field, then we may expect a high degree of atomic-spin polarization in the interaction region. On the other hand, if the electron-atom collisions take place in a low magnetic field, the atomic electron and nuclear spins are recoupled by the hyperfine interaction; the atomic state is described by its total angular momentum quantum number F, and the projection of F on the quantization axis, $M=m_J+m_I$. Under these circumstances, the atomic-spin polarization is degraded. This situation has been analyzed by Jaduszliwer, Bhaskar, and Bederson [6] for electron–rubidium-atom collisions. Cesium presents serious difficulties when using this approach. Because of the large value of its ground-state hyperfine splitting ($\Delta\nu_0\approx9.2$ GHz), "high" fields for cesium are indeed high, of the order of several kilogauss. Operating an electron gun with good momentum resolution at those magnetic-field levels becomes very difficult, but because

of the cesium high nuclear spin, $I=\frac{7}{2}$, performing the collision experiment in a low field after high-field state selection will seriously degrade the atomic-spin polarization. It is easy to show that in the limit in which eight atomic states are selected in very high fields by the inhomogeneous field magnet, the zero-field polarization of the beam will be 0.125.

Optical pumping of the cesium atomic beam [11] presents a way out of this quandary. Figure 4 shows the relevant zero-field Zeeman sublevels of the cesium $6S_{1/2}$ (ground) and $6P_{3/2}$ states, coupled by the D_2 transition at $\lambda\approx 852.1$ nm. A laser tuned to the $6S_{1/2},F=3$ to $6P_{3/2},F=4$ component of the D_2 line will depopulate the $F=3$ level of the ground state by hyperfine pumping. A second laser, tuned to the $6S_{1/2},F=4$ to $6P_{3/2},F=5$ component and emitting right-circularly-polarized (σ_+) light, will induce $\Delta M=1$ transitions and transfer all the atoms in the $F=4$ level to the $M=4$, $F=4$ state, which has unit amplitude for $m_J=\frac{1}{2}$, $m_I=\frac{7}{2}$ independently of the magnitude of the external magnetic field. In this way, a high degree of atomic-spin polarization can be achieved in low magnetic fields. Additionally, since spin polarization is accomplished by population transfer to the desired state, rather than by selection of a preexisting population, this technique makes a much more efficient use of the atomic beam. If the second laser beam is left-circularly polarized (σ_- light), $\Delta M=-1$ transitions will be induced, transferring the atoms to the $F=4$, $M=-4$ state having $m_J=-\frac{1}{2}$. The ease with which atomic polarization can be reversed simplifies the elimination of systematic errors. The availability of Al-Ga-As diode lasers at the $\lambda\approx 852$ nm wavelength makes this scheme particularly attractive.

Figure 5 shows how we have implemented the optical-spin-state-preparation scheme in our apparatus. We use two Mitsubishi ML2701 Al-Ga-As TJS (transverse junction stripe) single-mode diode lasers, mounted on thermally insulated copper blocks; laser temperatures were stabilized to better than 0.01 °C by a thermoelectric heater-cooler, and injection currents were controlled to better than 1 μA. The lasers are tuned to the $F=3$ to $F=4$ and $F=4$ to $F=5$ hyperfine components of the cesium D_2 transition, respectively. Their combined output beams, right- (left-) circularly polarized by quarter-wave plates, cross the atomic beam at right angles. A set of Helmholtz coils produces a weak magnetic field parallel to the laser beams to define the atomic quantization axis; photon absorptions induce $\Delta M=+1$ (-1) transitions in the atoms. After a number of excitation-decay cycles, most of the atoms in the beam are left in the $F=4$, $M=4$ (-4) state; the atomic beam has thus acquired a high degree of transverse spin polarization. In order to achieve axial spin polarization of the atomic beam, a second, axial field coil is located downstream from the Helmholtz coils. The coil geometries and currents are carefully adjusted so that their fringing fields match; an atom traveling along the axis of the apparatus is affected by a field rotating slowly from transversal in the optical-pumping region to axial at the exit of the coil arrangement, and rotates its quantization axis adiabatically to follow the field, without losing polarization. External coils, wound coaxially with the atomic beam, provide a weak field to define the quantization axis along the apparatus and prevent depolarization.

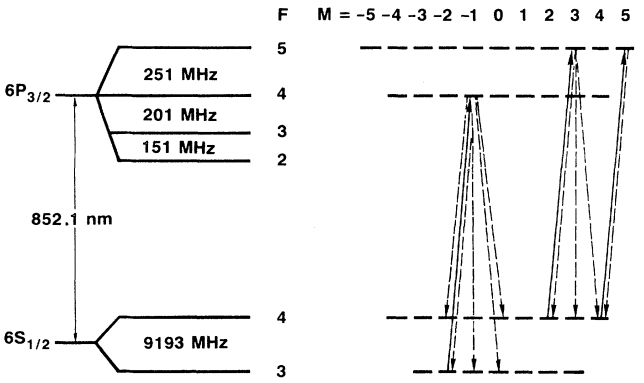

FIG. 4. Energy levels associated with the cesium D_2 transition (left) and optical-pumping scheme (right). Solid arrows, laser σ_+ photon absorptions; dashed arrows, spontaneous decays.

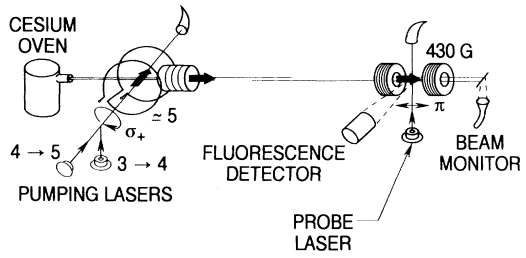

FIG. 5. Implementation of optical state preparation and state-sensitive detection. One of the state-preparation lasers depletes the $F=3$ states, and both lasers, in combination, transfer angular momentum until all the atoms in the beam are in the $|4,4\rangle$ state. The coils in the state-preparation region rotate the axis of quantization from transverse to axial. The probe laser stimulates fluorescence in the detection region; the 430-G field removes the Zeeman degeneracy.

Long-term stability of the atomic-beam polarization is achieved by locking the pumping lasers to the pumped atomic transitions. By modulating both lasers at incommensurate frequencies, the output of a single silicon photodetector monitoring the fluorescent emission from the optical-pumping region can be used to frequency-lock both lasers using conventional phase-sensitive detection techniques.

IV. STATE-SENSITIVE OPTICAL DETECTION

Consider a cesium atom, initially prepared in the $F=4$, $M=4$ state, which undergoes an elastic collision

with an electron. If there are no changes in the atomic-spin state, the atom will exit the interaction region in the same state. If there is a change in the atomic spin, the atom will exit the interaction region in a $M=3$ state, with $F=4$ or 3. Thus, in order to characterize fully the collision, we need to detect separately atoms in those three states. This can be done optically, by using a diode laser to excite transitions originating in each of those three levels of the ground state and detecting the atomic fluorescence. Separate detection of the $F=3$, $M=3$ state does not present a problem, since it is removed from the other ones by about 9.2 GHz. In order to distinguish between the $F=4$, $M=4$ and the $F=4$, $M=3$ states, laser-induced fluorescence detection takes place in a magnetic field of a few hundred gauss, as shown in Fig. 5. An iron-core electromagnet with 3.81-cm-diam polefaces, separated by a 0.95-cm gap, is energized by two 200-turn coils. A 0.64-cm axial bore allows the atomic beam to travel through the magnet. The magnetic field, parallel to the atomic beam, is homogeneous to within 5% in the region in which atomic and laser beams overlap, and in normal operation is set at $B\approx 430$ G. The laser beam is incident vertically, linearly polarized parallel to the field (π light) to stimulate $\Delta M=0$ transitions. Atomic fluorescence is monitored by a silicon photodetector (high-level signals) or a cooled photomultiplier with a GaAs photocathode (low-level signals).

The LIFB detector can be used in two different modes. In the spectral scan mode, the injection current into a third, dedicated probe laser is ramped up to scan the desired frequency range. In the single-state monitoring mode, the beam of one of the two frequency-locked pumping lasers is split. Most of the intensity is still directed into the optical-pumping region; the weaker, secondary beam is used as the probe laser after being shifted in frequency by an acousto-optical modulator to match the Zeeman transition of interest.

V. ZEEMAN SPECTRUM

In order to evaluate quantitatively the degree of polarization achieved by our technique, as well as to assign signature transitions to the $F=4$, $M=4$ and $F=4$, $M=3$ states, we calculated the positions and intensities of the emission lines expected in the Zeeman spectrum of the cesium D_2 transition at $B=430$ G after excitation by π-light absorption. The magnetic and hyperfine interaction corrections to the $6S_{1/2}$ (ground-) and $6P_{34/2}$ (excited-) state energies are determined by the Hamiltonian

$$H=(g_J J_z+g_I I_z)\mu_0 B+a\mathbf{I}\cdot\mathbf{J}\ , \tag{1}$$

where we have left out the small nuclear quadrupole contribution to the hyperfine interaction. At $B\approx 430$ G, $\mu_0 B/h\approx 0.6$ GHz, while the zero-field hyperfine splittings are about 9 and 0.2 GHz for the ground and excited states, respectively. Thus, transition frequencies could be calculated using the weak-field approximation for the ground state and the high-field approximation for the excited state. The results obtained using those approximations are off by up to 40 MHz for both ground and excited states. Since our experimental linewidth was only 38 Mhz, we were forced to calculate the exact transition frequencies by diagonalizing H in order to obtain reasonable agreement between measured and calculated Zeeman spectra. The corresponding matrices $\{H\}$ are 16×16 in the ground state and 32×32 in the excited state, but since $[\mathbf{F}_z,H]=0$, the only nonzero elements of $\{H\}$ are those coupling states of the same M.

For the ground state, having $J=\frac{1}{2}$, the secular equations are quadratic, and the results of the diagonalization of H are given by the Breit-Rabi formula [12]:

$$W(F,M)=\frac{-h\Delta\nu_0}{2(2I+1)}\pm\frac{h\Delta\nu_0}{2}\left[\frac{1+4Mx+x^2}{2I+1}\right]^{1/2}, \tag{2}$$

where $x=g_J\mu_0 B/h\Delta\nu_0$ and for the ground state of cesium, the Landé factor $g_J=2$. We have chosen te coupled representation $|F,M\rangle$, where the "+" solutions of Eq. (2) correspond to $F=4$ and the "−" solutions to $F=3$. The excited state has $J=\frac{3}{2}$ and diagonalizing $\{H\}$ requires solving quadratic, cubic, and quartic secular equations. The diagonalization was carried out in the uncoupled $|m_J,m_I\rangle$ representation, and the secular equations were solved using algebraic formulas for the roots. The relative π-transition probabilities for the shifted levels were calculated in the dipole approximation using the eigenvectors of $\{H\}$ for the $6S_{1/2}$ and $6P_{3/2}$ states. The results of those calculations for the transition manifold originating in the $F=4$ level of the ground state are shown in Fig. 6. We then calculated the expected $F=4$ manifold laser-induced-fluorescence spectrum at $B=430$ G by folding those transition probabilities with an empirical line shape given by the sum of a Gaussian and a Lorentzian function of equal widths; this profile incorporates the natural transition width, the laser line shape, the atomic-beam transverse Doppler width, and the detection-region

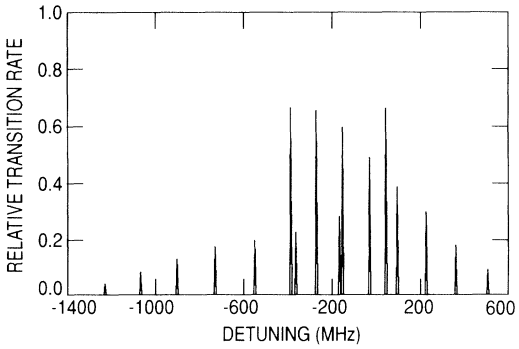

FIG. 6. π-transition rates and frequencies in the $F=4$ manifold of the cesium D_2 line in a 430-G magnetic field. Frequencies are given as detunings from the $F=4$ to $F=5$ zero-field hyperfine transition. Relative transition rates are given by the heights of the spikes. The individual transitions $|F,M\rangle$ to $|m_I,m_J\rangle$ are, from left to right: $|4,3\rangle$ to $|7/2,-1/2\rangle$, $|4,2\rangle$ to $|\frac{5}{2},-\frac{1}{2}\rangle$, $|4,1\rangle$ to $|\frac{3}{2}\rangle,-\frac{1}{2}\rangle$, $|4,0\rangle$ to $|\frac{1}{2},-\frac{1}{2}\rangle$, $|4,-1\rangle$, to $|-\frac{1}{2},-\frac{1}{2}\rangle$, $|4,4\rangle$ to $|\frac{7}{2},\frac{1}{2}\rangle$, $|4,-2\rangle$ to $|-\frac{3}{2},-\frac{1}{2}\rangle$, $|4,3\rangle$ to $|\frac{5}{2},\frac{1}{2}\rangle$, $|4,-3\rangle$ to $|-\frac{5}{2},-\frac{1}{2}\rangle$, $|4,2\rangle$ to $|\frac{3}{2},\frac{1}{2}\rangle$, $|4,1\rangle$ to $|\frac{1}{2},\frac{1}{2}\rangle$, $|4,-4\rangle$ to $|-\frac{7}{2},-\frac{1}{2}\rangle$, $|4,0\rangle$ to $|-\frac{1}{2},\frac{1}{2}\rangle$, $|4,-1\rangle$ to $|-\frac{3}{2},\frac{1}{2}\rangle$, $|4,-2\rangle$ to $|-\frac{5}{2},\frac{1}{2}\rangle$, and $|4,-3\rangle$ to $|-\frac{7}{2},\frac{1}{2}\rangle$.

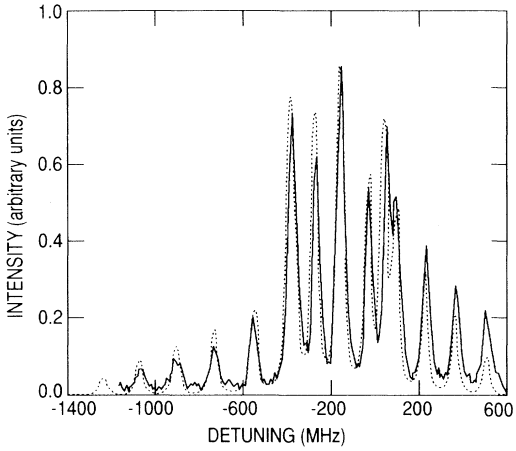

FIG. 7. Solid line, measured cesium-atomic-beam induced-fluorescence spectrum in a 430-G magnetic field for a π-polarized laser. Dashed line, induced-fluorescence spectrum calculated by folding the π-transition probabilities shown in Fig. 7 with an empirical line shape having 38 MHz FWHM.

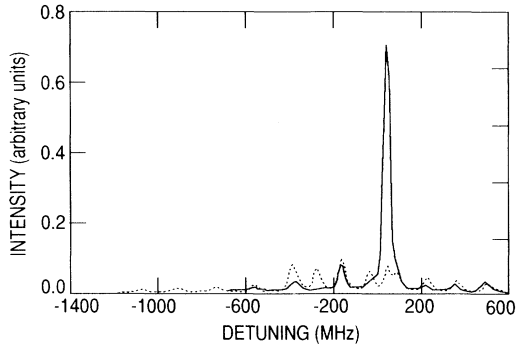

FIG. 8. Solid line, induced-fluorescence spectrum of a spin-polarized cesium atomic beam in a 430-G magnetic field for a π-polarized laser. The most intense transition originates from the $|4,-4\rangle$ state. The three low-intensity transitions at each side originate from the $F=4$, $M=-1$, -2, and -3 states, respectively. Dashed line, unpolarized cesium-atomic-beam induced-fluorescence spectrum obtained with a π-polarized laser (for reference purposes). Both spectra have been normalized to unit total intensity.

magnetic-field inhomogeneity. The transition width, 38 MHz full width at half-maximum (FWHM), was determined from the measured fluorescence spectrum, shown in Fig. 7. The results of the calculation, also shown in Fig. 7, are in excellent agreement with the measured spectrum. At the high-frequency end of the scan, the calculated spectrum seems to be less intense than the measured stimulated fluorescence; this was probably caused by an increasing laser output, assumed constant in the calculation.

VI. THE SPIN-POLARIZED CESIUM BEAM

The laser-induced-fluorescence spectrum at 430 G changes dramatically when the state-preparation lasers are turned on. In this case, both laser output beams are left-circularly polarized; thus, we expect the cesium atoms to leave the state-preparation region in the $F=4$, $M=-4$ state, having $m_J=-\frac{1}{2}$. Figure 8 shows the detected $F=4$ manifold laser-induced-fluorescence spectrum, as well as a reference spectrum obtained with the unpolarized beam. Both spectra have been normalized to unit total intensity. In the case of the unpolarized beam, a $\frac{7}{16}$ fraction of the total fluorescent intensity is emitted in the $F=3$ manifold, approximately 9 GHz away and not shown in the figure. No fluorescent emission in the $F=3$ manifold was detected in the case of the polarized beam, indicating a full population transfer to $F=4$ hyperfine states. Most of the detected fluorescence for the polarized beam originates from atoms in the $M=-4$ state, indicating a very large enhancement of its population. The fluorescence from the $M=-3$ state is left unchanged, the fluorescence from the $M=-2$ and $M=-1$ states is substantially reduced, and no fluorescence originating from the other states ($M=0,..,4$) is detected, indicating that those states are fully depopulated.

If $I_k(M)$ is the fluorescent intensity detected for transition "k," originating from state M, and $R_k(M)$ is the corresponding transition rate, the relative state populations are given by

$$\rho(M)=I_k(M)/R_k(M)\ . \tag{3}$$

Relative intensities and their estimated errors, obtained from data like those shown in Fig. 8; the corresponding relative transition rates, calculated as discussed in Sec. V; and the values of $\rho(M)$, obtained using Eq. (3) and normalized to unit sum; are given in Table I.

Since the coupled $|F,M\rangle$ states can be written in terms of the uncoupled $|m_I,m_J\rangle$ states as

$$|4,M\rangle=\langle\tfrac{7}{2},\tfrac{1}{2},4,M|\tfrac{7}{2},\tfrac{1}{2},M+\tfrac{1}{2},-\tfrac{1}{2}\rangle|M+\tfrac{1}{2},-\tfrac{1}{2}\rangle + \langle\tfrac{7}{2},\tfrac{1}{2},4,M|\tfrac{7}{2},\tfrac{1}{2},M-\tfrac{1}{2},\tfrac{1}{2}\rangle|M-\tfrac{1}{2},\tfrac{1}{2}\rangle\ , \tag{4}$$

TABLE I. Relative populations of $|4,M\rangle$ states in the polarized cesium beam. The numbers in parentheses indicate uncertainty levels and affect the last two significant figures.

M	Transition	$R_k(M)$	$I_k(M)$	$\rho(M)$
-1	$\|4,-1\rangle$ to $\|-\frac{1}{2},-\frac{1}{2}\rangle$	0.417	0.0138(06)	0.026(01)
-2	$\|4,-2\rangle$ to $\|-\frac{3}{2},-\frac{1}{2}\rangle$	0.500	0.0296(12)	0.047(02)
-3	$\|4,-3\rangle$ to $\|-\frac{5}{2},-\frac{1}{2}\rangle$	0.583	0.0727(27)	0.099(04)
-4	$\|4,-4\rangle$ to $\|-\frac{7}{2},-\frac{1}{2}\rangle$	0.667	0.695(14)	0.827(16)

the probabilities of measuring $m_J = \pm\frac{1}{2}$ for a cesium atom in the beam are

$$\rho(+\tfrac{1}{2}) = \sum_M |C(M,\tfrac{1}{2})|^2 \rho(M) \approx 0.035 \pm 0.001 ,$$
$$\rho(-\tfrac{1}{2}) = \sum_M |C(M,-\tfrac{1}{2})|^2 \rho(M) \approx 0.965 \pm 0.022 , \quad (5)$$

where the $C(M,m_J)$ are the Clebsch-Gordan coefficients defined by Eq. (4). The cesium-beam polarization is then given by

$$P = \rho(-\tfrac{1}{2}) - \rho(+\tfrac{1}{2}) \approx 0.930 \pm 0.023 . \quad (6)$$

The above results were obtained operating the LIFB detector in the spectral scan mode. As discussed in Sec. IV, it can also be operated in a fixed-frequency mode to monitor the fraction of the atomic beam in a given state. In this case, a fraction of the beam of the $F=4$ to $F=5$ state-preparation laser (locked to the zero-field 4-5 hyperfine transition frequency) is incident on an acousto-optic modulator. If, after preparing the atomic beam in the $|4,4\rangle$ state, we wish to detect $|4,3\rangle$ atoms, the acousto-optic modulator output beam is shifted in frequency by -274 MHz, to match the frequency of the $|4,3\rangle$ to $|\frac{1}{2},\frac{5}{2}\rangle$ transition in the 430-G detection-region field, and its polarization is adjusted to induce π transitions. The electron gun is turned on and of. When electrons are incident on the beam, some atoms undergo spin-changing collisions and arrive at the detection region in the $|4,3\rangle$ state, as indicated in Fig. 9. The nonzero signal while the electron gun is off is caused by incomplete optical pumping of the beam (as illustrated in Fig. 8) and by residual scattering of laser light within the detection chamber. Te signal rise time is determined by the detection electronics.

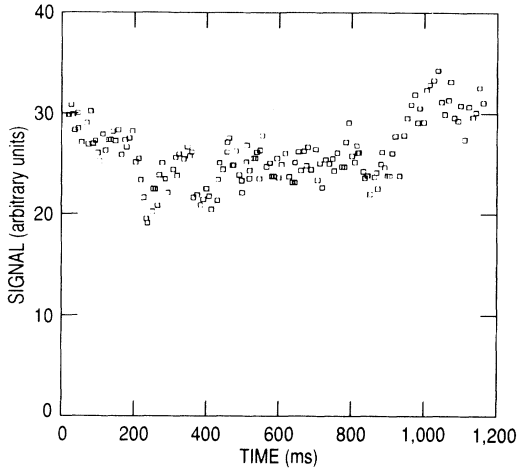

FIG. 9. Laser-induced fluorescence signal vs time. The laser is π-polarized and tuned to the $|4,3\rangle$ to $|\frac{1}{2},\frac{5}{2}\rangle$ transition, and the atomic beam is prepared in the $|4,4\rangle$ state. Spin-changing collisions with 1.3-eV electrons transfer some atoms to the $|4,3\rangle$ state, as shown by the changes in signal level at electron-gun turn-off ($t \approx 150$ ms) and turn-on $t \approx 850$ ms).

VIII. CONCLUSIONS

The combined use of optical-state preparation and state-sensitive detection is a powerful technique, which can be used to great advantage in atomic-recoil experiments to investigate the role of spin in atomic collisions. Optical-state preparation provides us with a highly polarized atomic beam, and removal of the atomic orientation degeneracy by performing optical detection in a magnetic field allows the full characterization of the atomic state after a collision. Since collision-recoiled atoms are detected via fluorescent emission, special care must be taken to prevent scattered laser light from corrupting the detector signal. All of the other technical problems associated with performing such experiments have been essentially solved.

ACKNOWLEDGMENT

This work was supported by the Aerospace Sponsored Research Program.

[1] Ramsauer, Ann. Phys. (Leipzig) **64**, 513 (1921); **66**, 545 (1921).
[2] J. Kessler, in *Advances in Atomic and Molecular Physics,* edited by D. Bates and B. Bederson (Academic, San Diego, 1991), p. 81.
[3] P. G. Burke and J. F. B. Mitchell, J. Phys. B **7**, 214 (1974).
[4] P. S. Farago, J. Phys. B **7**, L28 (1974).
[5] J. J. McClelland, M. H. Kelley, and R. J. Celotta, Phys. Rev. Lett. **58**, 2198 (1987).
[6] B. Jaduszliwer, N. Bhaskar, and B. Bederson, Phys. Rev. A **14**, 162 (1976).
[7] G. Baum, B. Granitza, S. Hesse, B. Leuer, W. Raith, K. Rott, M. Tondera, and B. Witthuhn, Z. Phys. D **22**, 431 (1991).
[8] R. E. Collins, M. Goldstein, B. Bederson, and K. Rubin, Phys. Rev. Lett. **19**, 1366 (1967).
[9] B. Jaduszliwer and Y. C. Chan, Phys. Rev. A **45**, 197 (1992).
[10] H. M. Brash, D. M. Campbell, P. S. Farago, A. G. A. Rae, H. C. Siegmann, and J. S. Wylkes, Proc. R. Soc. Edinburgh, Sect. A **68**, 159 (1968/69), Pt. II.
[11] R. N. Watts and C. E. Weiman, Opt. Commun. **57**, 45 (1986).
[12] G. Breit and I. I. Rabi, Phys. Rev. **38**, 2082 (1931).